DOI: https://doi.org/10.36811/jca.2020.110006 **JCA: August-2020: Page No: 10-21**

Universal Journal of Chemistry and Applications

Research Article **Open Access**

A Dft Pursuit on Tandem Cycloaddition-Cycloreversion of 2-Pyrone and 1,4-Oxazinone with Strained Alkynes

Akilandeswari L[1], Kalpana P[1] and Venuvanalingam P[2]*

[1]Department of Chemistry, Sri Sarada College for Women (Autonomous), Salem-636 016, Tamilnadu, India
[2]School of Chemistry, Bharathidasan University, Trichirappalli, Tamilnadu, India

***Corresponding Author:** Venuvanalingam P, School of Chemistry, Bharathidasan University, Trichirappalli, Tamilnadu, India, Email: venuvanalingam@yahoo.com

***Received Date:** Jul 29, 2020 / **Accepted Date:** Aug 27, 2020 / **Published Date:** Aug 29, 2020*

Abstract

2-Pyrone (2P) and 1,4-oxazinone (OXZ) react with strained alkynes viz., cyclohexyne (SA1), benzyne (SA2) and pyridyne (SA3) through concerted cycloaddition-cycloreversion reaction. All the reactions have been scanned and the activation parameters, FOE, deformation energies and variation in aromaticity computed at B3LYP/6-31g(d) level.The obtained results have been compared with that of acetylene. In SA1,faster cycloadditionis explained by its strain, in addition,aromatic gain is accountable to enhance the rate of cycloaddition in SA2 and SA3.

Cite this article as: Akilandeswari L, Kalpana P, Venuvanalingam P. 2020. A Dft Pursuit on Tandem Cycloaddition-Cycloreversion of 2-Pyrone and 1,4-Oxazinone with Strained Alkynes. J Chem Appl. 2: 10-20.

Introduction

Tandem cycloaddition-cycloreversion reactions are synthetically important to produce enormous natural products. One might reasonably expect that increased strain will lead to enhanced reactivity of a molecule and thus molecules become good candidates here to perform tandem reactions. Literature apparently shows the effect of ring size on the reactivity of cyclic alkynes [1-7]. Other strained alkynes (SAs) include arynes which are the reactive intermediates derived from substituted arenes that participate in some aromatic nucleophilic substitutions [8,9] and some cycloaddition reactions [10]. The most extensively studied aryne is benzyne which is known to undergo [4+2] cycloaddition with dienes like oxazole and thiophene derivatives [11-13]. Cyclohexyne has been reported to undergo tandem cycloaddition-cycloreversion with 2-pyrone to form tetrahydronaphthalene. This strategy when operated with some complex pyrones yielded analogues of planar frame work of dynemicin-A [14]. The effect of heteroatom on tandem cycloaddition-cycloreversion of 2-pyrone and 1,4-oxazinone with hetero alkynes has also been explored theoretically [15,16]. On the other hand,addition of benzynes and pyridynes with 2-pyrone have so far not been reported

DOI: https://doi.org/10.36811/jca.2020.110006 JCA: August-2020: Page No: 10-21

experimentally. This is the stimulus to have the aim of this work i.e., (i) to monitor the effect of strained triple bond of cyclohexyne and arynes over the tandem cycloaddition and cycloreversion, (ii) the effect of strain and aromatic gain on the reactivity in benzyne and pyridyne and (iii) the effect of strain, aromatic gain and the effect of hetero atom in pyridyne reaction. This study discusses the computed results such as activation parameters, FO analyses, deformation energies, variation in aromaticity along the reaction coordinates of the transition states formed during the tandem cycloaddition-cycloreversion reaction of 2P and OXZ with strained alkynes viz., cyclohexyne (SA1), benzyne (SA2) and pyridyne (SA3) and compared with that of acetylene.

Computational Methods

All the reactions have been modelled and scanned using Gaussian 98 program [17] at B3LYP[18,19]/6-31G (d) level. The magnetic susceptibility isotropy has been calculated by computing the NMR shielding tensors at B3LYP/6-311+G (2d, p) using IGAIM method [20,21] which is a slight variation of CSGT [20,21] method. Natural bond orbital (NBO) calculations have been performed. For both the cycloaddition and cycloreversion processes, the variation in magnetic susceptibility isotropy (χ_{iso}) along the reaction coordinate has been monitored. Change in aromaticity during the reactions has been computed.

Results and Discussion

Cycloaddition and cycloreversion of 2P and OXZ with strained alkynes SA1, SA2 and SA3 form benzo fused aromatics which are illustrated in Scheme 1 and 2. The relative free energy profile for the sequence of 2P and OXZ with strained alkynes are represented in figure 1-6 along with the optimized geometries and notable bond distances. There is the possibility of two extruding groups from the cycloadduct viz., CO_2 and HCN in the case of cycloreversion of strained alkyne with OXZ. When SA3 is the dienophile there are 2 regioisomeric adducts possible, denoted as Regio 1 and Regio 2 in Scheme 1(c)& 2(c).

A. Energetics

2P-SAs reactions

The free energy profile in figure 2-5 and thermochemical parameters in table 4 indicate that 2P-SAs cycloadditions are much faster (barrier lying between 13-16 kcal mol^{-1}) than 2P-Ace reaction ($\Delta G^{\ddagger}$ for 2P-Ace cycloaddition is 36.84 kcal mol^{-1}). Among strained alkynes considered, SA2 reacts faster ($\Delta G^{\ddagger}$ =13.30 kcal mol^{-1}) followed closely by SA3 ($\Delta G^{\ddagger}$ =13.92 kcal mol^{-1}) and then SA1which has relatively higher barrier by about 3 kcal mol^{-1} ($\Delta G^{\ddagger}$ =16.70 kcal mol^{-1}). In 2P-SA3 reaction, Regio 1 (R1)& Regio 2 (R2) pathways are closely lying with a very negligible difference (0.04 kcal mol^{-1}). Hence the figure 4 shows the geometries of only R2 and relative free energies of the systems on R1 are given in parenthesis.

The cycloaddition of the three SAs lead to highly stable and exothermic cycloadducts viz., A1, A2 and R1A3 & R2A3. The exothermicity of these cycloadducts are (ΔH_r= -65.55, -80.03, -77.27 kcal mol^{-1} of A1, A2 and R2A3 respectively) two to three fold greater than that of simple acetylene (ΔH_r= -29.38 kcal mol^{-1}) due to two factors: (i) Release of strain in the triple bond (ii) Aromaticity gain in the adduct. It is revealed by the formation of strainless aromatic benzene and pyridine fused with bicyclic lactones A2 and A3 respectively, in 2P-SA2 and 2P-SA3 reactions. In contrast, there is only strain release, not the aromatic gain in 2P-SA1 cycloaddition. The barrier to cycloreversion shown in table 1. indicates that A1 extrudes CO_2 faster and is comparable with that of 2P-Ace reaction. On the other hand, A2 and A3 ($\Delta G^{\ddagger}$ =15.95 kcal mol^{-1} and 16.91 kcal mol^{-1}) have their cycloreversion barrier about 4-5 kcal mol^{-1} higher than 2P-SA1 reaction. This is ascertained to the excessive thermodynamic stability of the cycloadduct. Extra stabilization

DOI: https://doi.org/10.36811/jca.2020.110006 JCA: August-2020: Page No: 10-21

in A2 and A3 due to aromatic gain also results in higher barrier to cycloreversion.

OXZ-SAs reactions

The barrier to cycloaddition is reduced for OXZ-SAs reactions also, as observed in OXZ-Ace. Reduction in barrier in OXZ-SAs reactions ($\Delta G^{\ddagger}$=4.5 kcal mol^{-1}, 3.3 kcal $mol^{-1}$and 2.8 kcal mol^{-1} for SA1, SA2 and SA3 respectively) are less than that of simple alkyne case ($\Delta G^{\ddagger}$=7 kcal mol^{-1}). Nitrogen in the system facilitates the reaction due to fewer aromatic loss and its remote location,from the reacting triple bond in SA3, affects the barrier to the least extent. Now the reactivity order of the SAs with OXZ is SA2>SA3>SA1>Ace. The reduction in free energy of activation of the OXZ-SAs reaction presented in Table 2. It is ascribed to a much lesser activation enthalpy compared to 2P-Ace case shown in Table 1. It is notable that $\Delta H^{\ddagger}$ for the OXZ-SA2 and OXZ-SA3 reactions are slightly negative. $\Delta S^{\ddagger}$ for cycloaddition and cycloreversion resemble that of 2P-Ace and 2P-SAs reactions. In OXZ-SAs reactionsSA2 and SA3 form cycloadduct A4 and A5, whereas SA3 makes two regioisomeric adducts R1A6 and R2A6. Their stability order is A4<R1A6<A5<R2A6. Out of two pathways, similar to OXZ-Ace reaction, CO_2 extrusion is facile than HCN elimination and the difference their barriers is nearly 15-20 kcal mol^{-1}. Cycloreversions of A4, A5, R1A6 and R2A6 ($\Delta G^{\ddagger}$=14.33, 19.69, 19.37 and 21.34 kcal mol^{-1} respectively) are similar to 2P-Ace reaction.

Frontier Orbital Analyses

Strained alkynes have their HOMO raised and LUMO lowered than simple alkyne and hence show higher reactivity. FOE gaps in figure 7 show that the 2P-SA1 cycloaddition follows Inverse Electron Demand (IED), similar to 2P-Ace. Added unsaturations and hetero atom stabilize the FOs of SA2 and SA3 respectively. As their LUMOs are lowered, SA2 and SA3 react by normal electron demand (NED) type. These FOE results are supported by Q_{CT} at the dienophile in the 2P-SA2 and 2P-SA3 reactions whereas 2P-SA1 reaction contradicts the FOE prediction, as its Q_{CT} is negative. In OXZ-SAs reactions, cycloaddition of OXZ-SA1 is IED type, similar to 2P-SA1 and is supported by Q_{CT}. Reduction in FOE gap indicates fall in the activation barrier to OXZ-SA1 cycloaddition. OXZ-SA2 reaction is IED, in contrast Q_{CT} predicts it to be a NED type as -0.028 charge is on the dienophile. FOE gaps show OXZ-SA2 reaction is neutral electron demand type whereas its Q_{CT} value is -0.047, representing it to be NED. In OXZ-SA3 and 2P-SA1 reactions, FOE gaps predicts IED type while Q_{CT} values indicate as NED type reactions.

Effect of strain on reactivity

The barrier to cycloaddition for 2P-SAs is less than 2P-Ace reaction, recognizing the reactivity (deformation energy) promoted by the strained triple bond. The deformation energies of diene and dienophile (DE1and DE2 respectively), in the corresponding transition state are presented in table 3. In 2P-Ace reaction, both diene and dienophile are largely deformed whereas drastically reduced in 2P with strained alkynes which has the order as SA1>SA3>SA2. This aligns their barrier trend.Further, in OXZ reaction N in the embedded diene still reduces the deformation energy of both diene and dienophile.

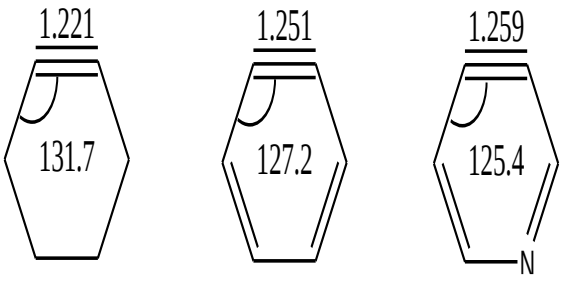

Figure 1

The bond length elongation and deviation of angle in SAs shown in figure 10 agree with the trend in the reactivity. The barrier to cycloaddition is also dependent on the

DOI: https://doi.org/10.36811/jca.2020.110006 JCA: August-2020: Page No: 10-21

difference between the initial angles (viz., C8-C7-C12 and C7-C8-C9) in the alkyne and that of cycloadduct. Comparison of variation of C8-C7-C12 and C7-C8-C9 angles for the strained and simple alkyne with 2P along the reaction coordinate of cycloaddition TS is presented in figure 11. Greater the difference in angle, greater is the barrier and variation in angle is sharp in 2P-Ace whereas very slight in 2P-SAs reactions.

Variation of aromaticity along the reaction coordinates

Aromatic gain during the reactions will definitely influence the rate. Among the three SAs involved reactions, SA2 and SA3 form benzo and pyrido-fused cycloadducts respectively, while SA1does not. The variation of aromaticity has been monitored by plotting the χ_{iso} along the reaction coordinate of both cycloaddition and cycloreversion of TSs. These plots of 2P-SA1 and 2P-SA2 reactions are collected in figures 14&15 respectively. Similar plots of 2P-SA3 and OXZ-SAs have not been done, as it resembles that of 2P-SA2.

2P-SA1 reaction

The change in χ_{iso} of TS1 (in the region -1 to +1 $(amu)^{1/2}$ .Bohr) along the reaction coordinate is shown in figure 12(a). The curve indicates a continuous aromatic enhancement during the reaction, at the TS there is an increase (more negative χ_{iso} value representing aromatic enhancement) while the rate of aromaticity gain is gradually decreased. Figure 6 (b) & (c) show the variation of χ_{iso} of pyrone and cyclohexyne ring, indicating a decrease in negative χ_{iso} till TS followed by a steeper increase. It explains both the rings lose aromaticity during cycloaddition and hence the continual aromaticity increase in plot 6(a) is due to the pericyclic closed curve formed. In this case, gain in aromaticity even after the TS can be explained as follows. The reacting LUMO of SA1 is perfectly oriented for good overlap with incoming diene. Also the change in angles are less along the reaction coordinate as the SA1is nearly close to its geometry in the adduct. This is reflected in deformation energy (DE2) TS being very low for the SAs in general. Therefore, even after the TS, deformation of SA1 will be necessarily low thereby increase in the aromaticity. During cycloreversion, except for the absolute value of χ_{iso} which is very high due to the fused benzene, the trend remains the same. Both plots 6 (d) & (e) show a linear increase in χ_{iso} owing to the formation of tetrahydronaphthalene (P1) after CO_2 extrusion and hence the aromaticity of newly formed ring dominates the scenario.

2P-SA2 reaction

The variation of χ_{iso} during 2P-SA2 reaction shown in figure 7 indicates a profile similar to 2P-SA1 reaction. In this case, a continual linear increase in χ_{iso} even after the TS is observed. It is ascribed to the aromatic gain by the benzene ring (plot 7 (c)). The pyrone ring fragment (plot 7 (b)) loses aromaticity which is compared with a low DE1 in 2P-SA2 reaction. Hence the least deformation of the pyrone ring is reflected in aromaticity monitored as variation in χ_{iso}. During cycloreversion, negative value of χ_{iso} increases due to CO_2 extrusion to form naphthelene. Therefore, unlike in a typical pericyclic reaction, there is a continual increase of aromaticity.

DOI: https://doi.org/10.36811/jca.2020.110006 **JCA: August-2020: Page No: 10-21**

Table 1: Thermochemical activation parameters of 2P-SAs reactions. (ΔG, $\Delta G^{\ddagger}$, $\Delta H^{\ddagger}$ and ΔH_r are in kcal mol^{-1} and $\Delta S\&\Delta S^{\ddagger}$ in cal $K^{-1}mol^{-1}$).

Cycloaddition						Cycloreversion				
DP	Activation parameters			Reaction parameters		Activation parameters			Reaction parameters	
	$\Delta G^{\ddagger}$	$\Delta H^{\ddagger}$	$\Delta S^{\ddagger}$	ΔH_r	ΔG_r	$\Delta G^{\ddagger}$	$\Delta H^{\ddagger}$	$\Delta S^{\ddagger}$	ΔH_r	ΔG_r
SA1	16.7	4.48	-41.01	-65.55	-50.24	11.82	12.13	1.04	-50.67	-63.04
SA2	13.3	1.73	-38.83	-80.03	-65.04	15.95	16.42	1.58	-41.7	-54.13
SA3 (R1)	13.96	1.99	-40.17	-77.02	-61.74	16.91	17.69	2.62		
(R2)	13.92	1.93	-40.24	-77.27	-61.98	15.84	16.34	1.68	-42.8	-54.99

Table 2: hermochemical activation parameters of OXZ-SAs reactions. (ΔG, $\Delta G^{\ddagger}$, $\Delta H^{\ddagger}$ and ΔH_r are in kcal mol^{-1} and $\Delta S\&\Delta S^{\ddagger}$ in cal $K^{-1}mol^{-1}$).

Cycloaddition						Cycloreversion								
DP	Activation parameters			Reaction parameters		CO2 Elimination					HCN Elimination			
						Activation parameters			Reaction parameters		Activation parameters			Reaction parameters	
	$\Delta G^{\ddagger}$	$\Delta H^{\ddagger}$	$\Delta S^{\ddagger}$	ΔH_r	ΔG_r	$\Delta G^{\ddagger}$	$\Delta H^{\ddagger}$	$\Delta S^{\ddagger}$	ΔH_r	ΔG_r	$\Delta G^{\ddagger}$	$\Delta H^{\ddagger}$	$\Delta S^{\ddagger}$	ΔH_r	ΔG_r
SA1	12.14	-0.17	-40.17	-60.71	-45.7	14.33	14.7	1.24	-47.3	-59.7	29.25	30.43	3.96	-0.32	-13.35
SA2	10.27	-0.87	-37.38	-88.69	-73.61	19.69	20.23	1.81	-38.34	-50.83	39.17	40.64	4.9	-15.96	-2.69
SA3 (R1)	11.29	-0.34	-39.03	-84.89	-69.52	19.37	19.95	2.05	-39.3	-69.34	39.24	40.71	4.32	-14.42	-1.09
(R2)	11.16	-0.54	-39.26	-85.29	-69.93	21.34	21.89	1.85	-38.28	-51.78	39.58	40.98	4.07	-17.58	-4.28

DOI: https://doi.org/10.36811/jca.2020.110006 **JCA: August-2020: Page No: 10-21**

Table 3: Deformation energy of dienes (2P & OXZ) (DE1) and dienophile (Ace, SA1, SA2, SA3) (DE2) components in the concerted cycloaddition transition states in (kcal mol^{-1}) and quantum of charge transferred to dienophile

Diene	DE1	Dienophile	DE2	Q_{CT}
2P	19.79	Ace	11.74	0.024
	7.80	SA1	0.77	-0.001
	4.37	SA2	0.60	-0.069
	4.71	SA3	0.67	-0.090
OXZ	16.86	Ace	9.33	0.052
	4.65	SA1	0.39	0.029
	1.90	SA2	0.23	-0.028
	2.33	SA3	0.27	-0.047

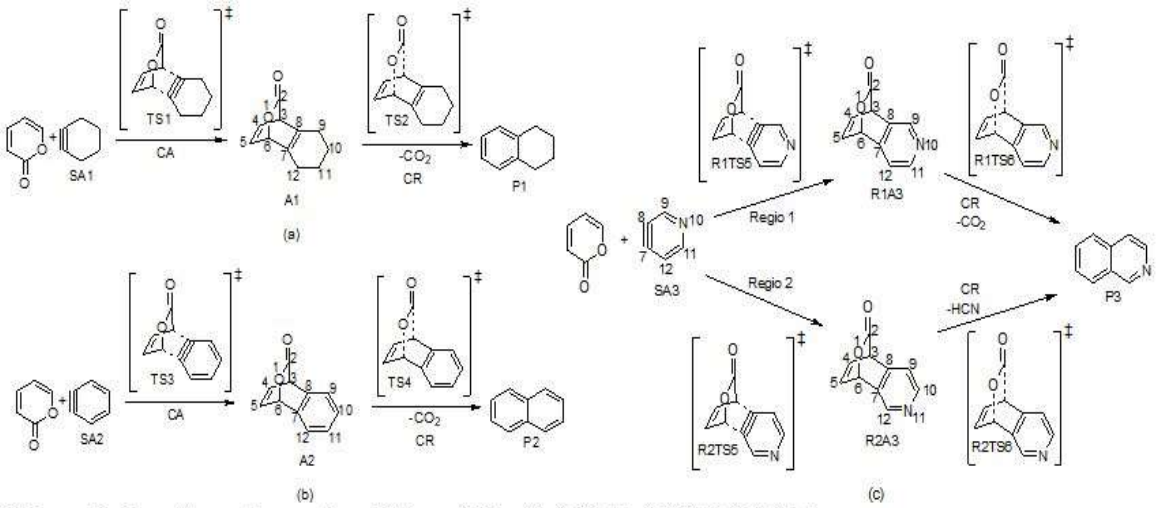

Scheme 1: Reaction pathways for addition of 2P with (a) SA1 (B) SA2 (C) SA3.

DOI: https://doi.org/10.36811/jca.2020.110006 **JCA: August-2020: Page No: 10-21**

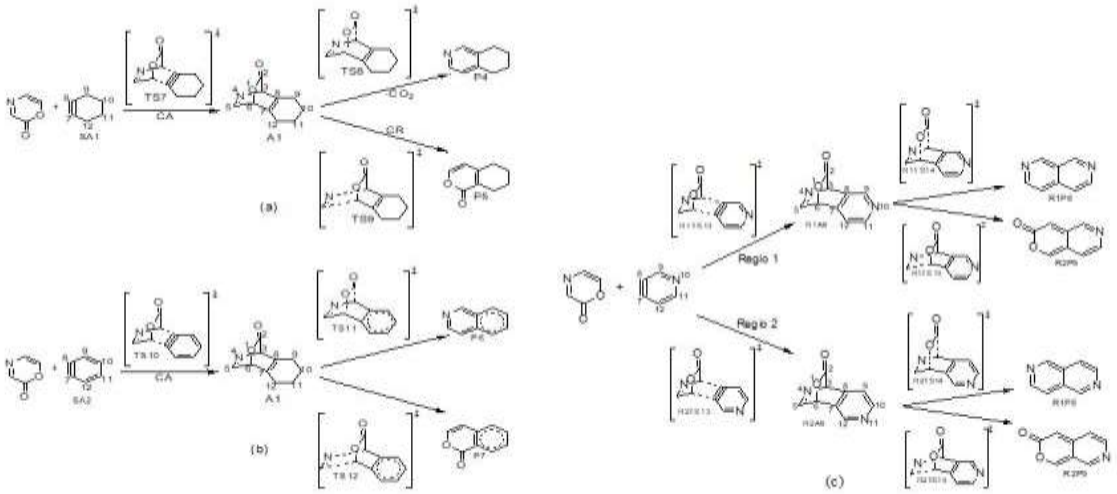

Scheme 2: Reaction pathways for addition of OXZ with (a) SA1 (B) SA2 (C) SA3.

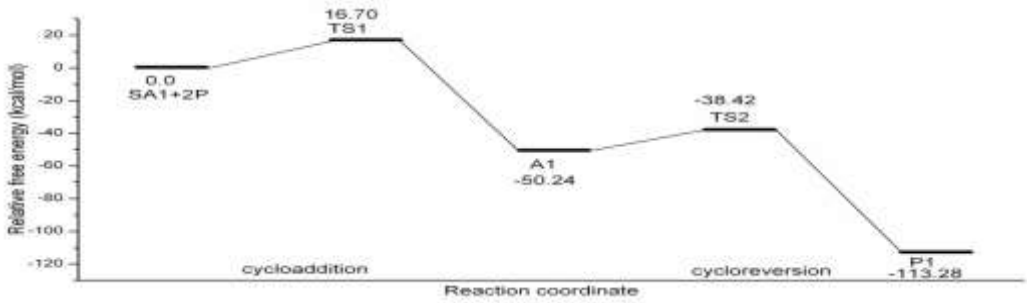

Figure 2: Schematic free energy profile of 2P-SA1 reaction computed at B3LYP/6-31G (d) level.

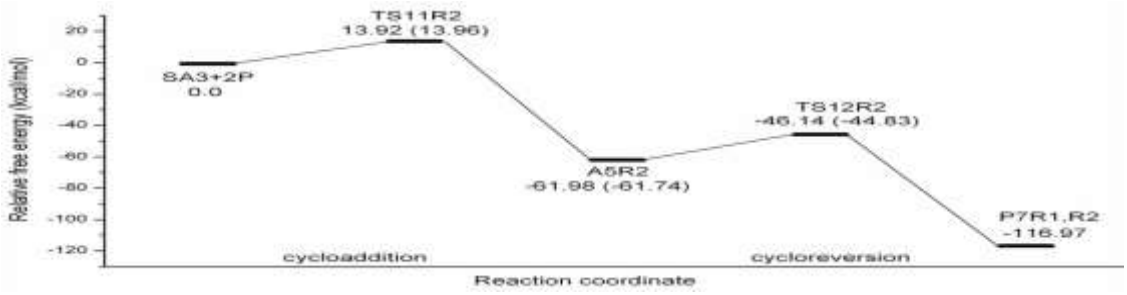

Figure 3: Schematic free energy profile of 2P-SA3 reaction computed at B3LYP/6-31G (d) level (The values in the brackets refer to Regio 1 reaction).

DOI: https://doi.org/10.36811/jca.2020.110006 JCA: August-2020: Page No: 10-21

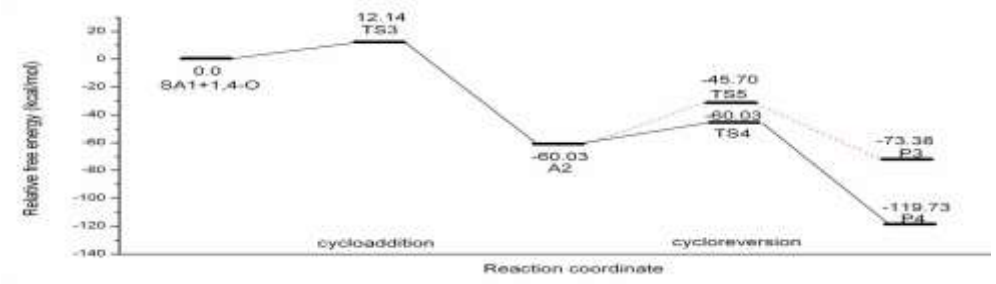

Figure 4: Schematic free energy profile of OXZ-SA1 reaction computed at B3LYP/6-31G (d) level.

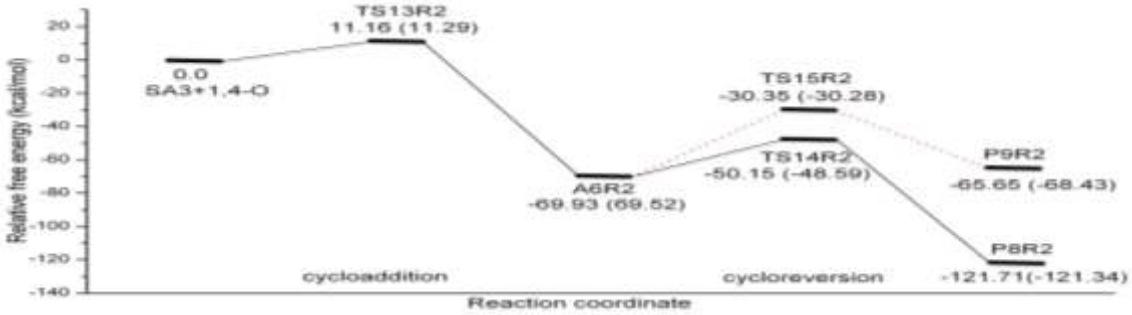

Figure 5: Schematic free energy profile of OXZ-SA3 reaction computed at B3LYP/6-31G (d) level (The values in the brackets refer to Regio 1 reaction).

DOI: https://doi.org/10.36811/jca.2020.110006 **JCA: August-2020: Page No: 10-21**

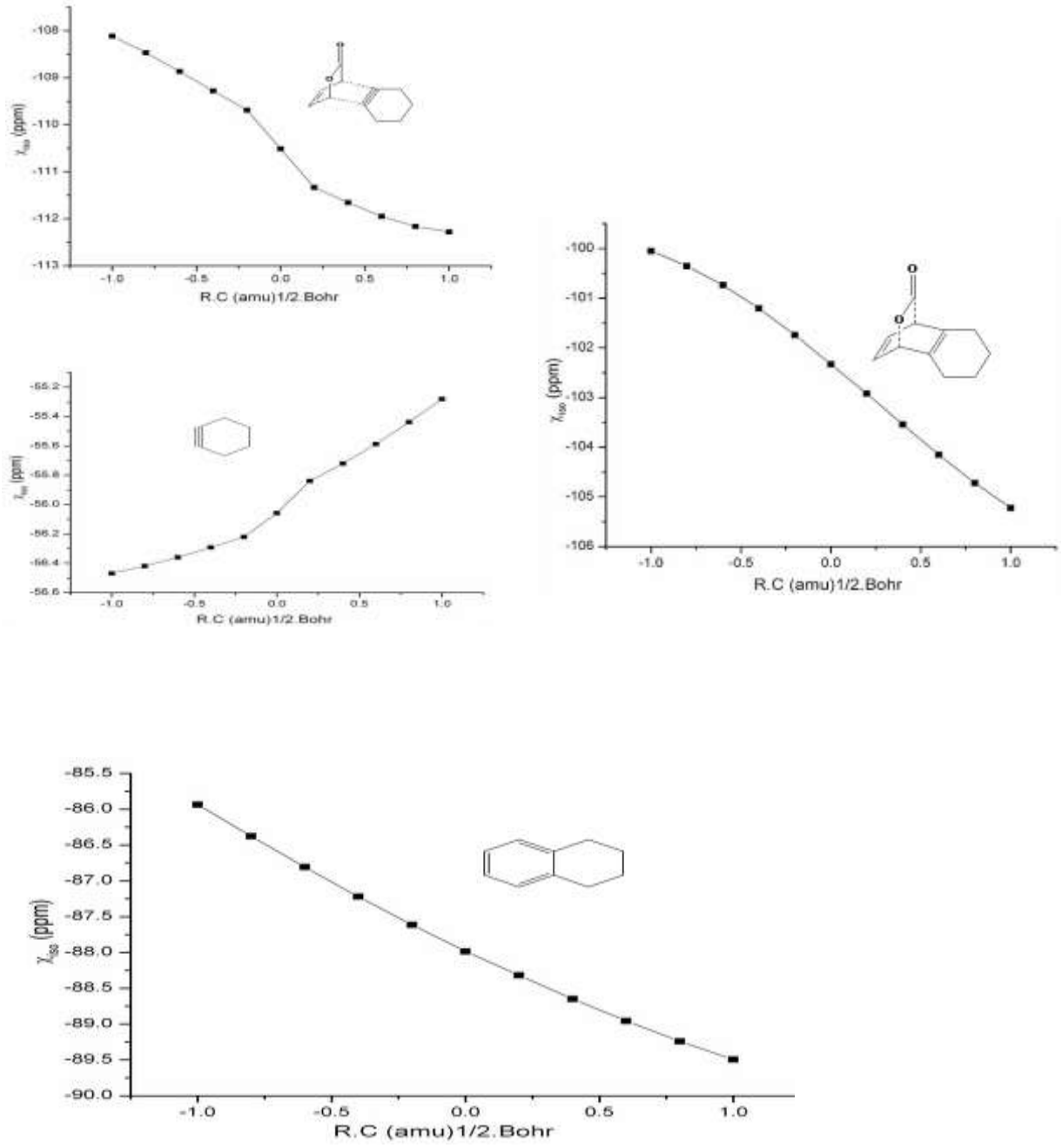

Figure 6: Variation of magnetic susceptibility isotropy along the reaction coordinate of 2P-SA1reaction around (a) TS1 (b) pyrone ring of TS1 (c) cyclohexyl ring of TS1 (d) TS2 (e) tetrahydronaphthalene ring of TS2.

DOI: https://doi.org/10.36811/jca.2020.110006 JCA: August-2020: Page No: 10-21

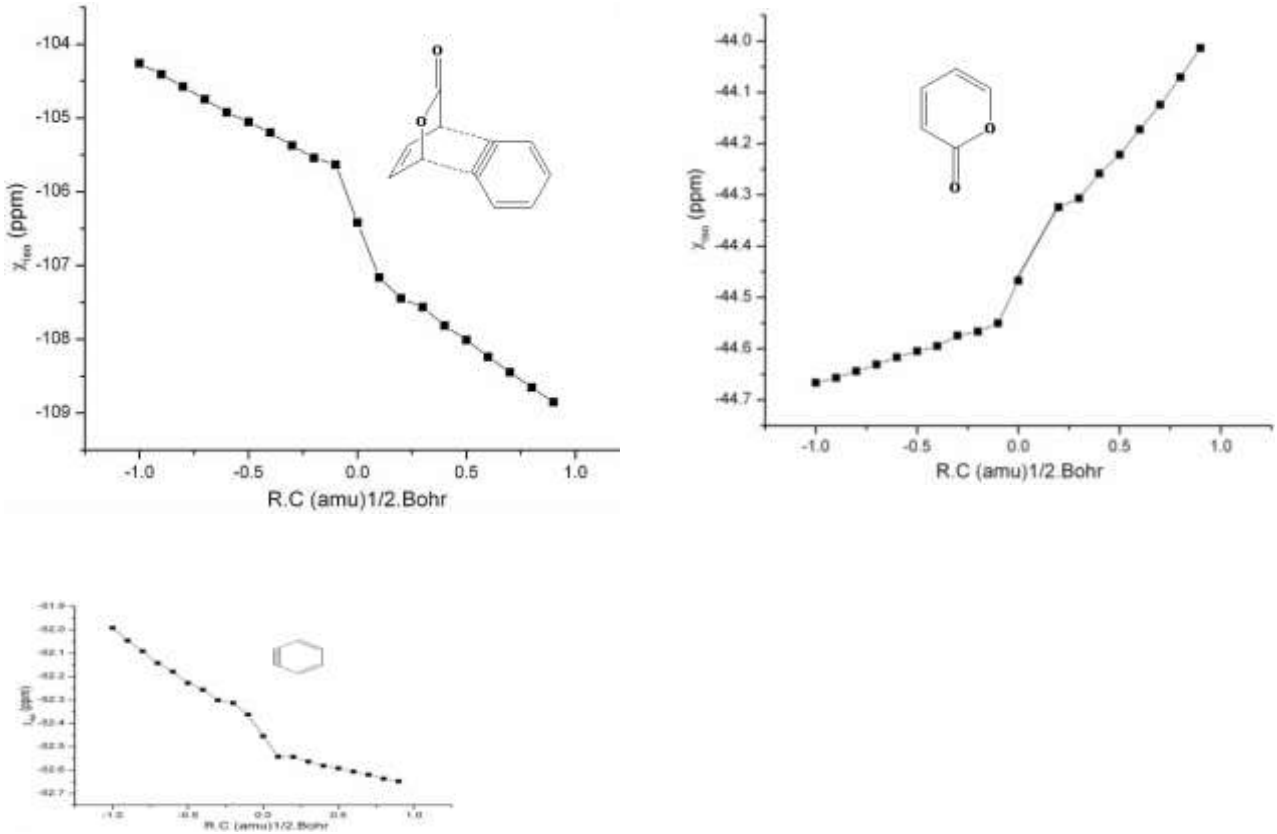

Figure 7: Variation of magnetic susceptibility isotropy along the reaction coordinate of 2P-SA1reaction around (a) TS1 (b) pyrone ring of TS1 (c) benzene ring of TS1 (d) TS2 (e) naphthalene ring of TS2.

Conclusions

Tandem cycloaddition-cycloreversion of 2-pyrone and 1,4-oxazinone with strained alkynes namely cyclohexyne(SA1), benzyne(SA2) and pyridine(SA3) occurs through concerted mechanism with slight asynchronicity due to the unsymmetric diene. Among the strained alkynes, benzyne reacts faster and pyridyne follows it, while cyclohexyne does slowly. All the three strained alkynes react extremely faster than Acetylene (Ace). Cycloreversion of 2P-SA1 adduct is comparable to 2P-Ace. In SA2 & SA3, cycloreversion is the rate determining step owing to the larger stability of adducts by strain release and aromatic gain by small $\Delta H^{\ddagger}$ and magnetic anisotropy variation. Aza diene cycloadds faster with strained alkynes whereas cycloreverts slower than the non aza diene. Deformation analysis explains extremely faster cycloaddition of SA1 with 2P & OXZ is due to its strain. In SA2 & SA3, strain and aromatic gain enhance the rate of cycloaddition and is demonstrated by variation of aromaticity. FO analysis shows the normal and inverse electron demands in these dienophiles especially in benzyne and pyridyne. Overall, the study proves that release of strain and aromaticity gain governs the tandem reaction of strained alkynes.

DOI: https://doi.org/10.36811/jca.2020.110006 **JCA: August-2020: Page No: 10-21**

References

1. Wittig G. 1942. Phenyl-lithium, der Schlüssel zu einer neuen Chemie metallorganischer Verbindungen Naturw is sensch aften. 30: 696. Ref.: shorturl.at/jCDKY
2. a) Hoffmann RW. Dehydrobenzene, Cycloalkynes. 1967 Academic Press: New York. b) Krebs A. 1969. In Chemistry of Acetylenes, Marcel Dekker: New York. c) LeNoble WJ. 1974. Highlights of Organic Chemistry; Marcel Dekker: New York. d) Greenberg A, Liebmann JF. 1978. Strained Organic Compounds; Academic Press: New York. e) Wittig G. 1963. Pure Appl. Chem. 7: 173.
3. a) Nakagawa M. 1978. in The Chemistry of the Carbon-Carbon Triple Bond. Wiley: New York. b) Montgomery, L, Roberts JDJ. 1960. Am. Chem. Soc. 82: 4750, Wittig G, Wenlich J, Wilson *E. Chem. Ber*. 1965. 98: 458. Gassman, P.; Gennick, I. *J. Am. Chem. Soc*. 1980, 102, 6863.
4. Montgomery LK, Applegat LEJ**.** 1967. Am. Chem. Soc. 89: 5305.
5. Allinger N L, Meyer AY. 1975. Conformational analysis-CIX: Applications of molecular mechanics to the structures and energies of alkynes. Tetrahedron. 31: 1807. Ref.: shorturl.at/cprMW
6. Schmidt H, Schweig A. Krebs A. 1974. Splitting of the degenerate acetylenic πmos; a probe for ring strain. Tetrahedron Lett. 16: 1471. Ref.: shorturl.at/ftGS6
7. a) Bunnett JFJ. 1961. Chem. Educ. 38: 278. b) Wittig, G. 1961 Angew. Chem. Int. Ed. Engl. 4: 731.
8. Gilchrist TL, 1983. in The Chemistry of functional groups, Supplement C. Wiley: New York.
9. Bryce MR, Vernon JM. 1981. Reactions of Benzyne with Heterocyclic Compounds. Adu. Heterocycl. Chem. 28: 183. Ref.: shorturl.at/htQWX
10. Dolbier WR, Loma D, Garza T, et al. 1972. Dimerizations of methylenecyclopropanes Harmon. Tetrahedron. 28: 3185. Ref.: shorturl.at/glIJP
11. van der Plaas HC, Roeterdink F. 1983. in The Chemistry of functional groups, Supplement C. Wiley: New York.
12. Whitney SE, Winters M, Rickborn B*J*. 1990. Org. Chem. 55: 929.
13. Thiemann T, Fujii H, Ohira D, et al. Cycloaddition of thiophene S-oxides to allenes, alkynes and to benzyne. 2003. New J.Chem. 27: 1377. Ref.: shorturl.at/csHV3
14. Atanes N, Escudero S, Pẽrez D, et al. Generation of cyclohexyne and its Diels-Alder reaction with α-pyrones. 1998. Tetrahedron Lett. 39: 3039. Ref.: shorturl.at/kqrBE
15. Akilandeswari L. Ph.D thesis. 2007. Bharathidasan University Tiruchirappalli,https://shodhganga.inflibnet.ac.in/jspui/handle/10603/115127.
16. Akilandeswari L, Kalpana P. 2018. International Journal of Chemistry Studies. 2: 12.
17. Frisch MJ, et al. 1998. Gaussian 98 (Revision A.9), Gaussian, Inc. Pittsburgh, PA.
18. Becke AD. 1993. Density-functional thermochemistry. I. The effect of the exchange-only gradient correction. Chem. Phys. 98: 5648. Ref.: shorturl.at/cnCR0
19. Lee C, Yang W, Parr RG. 1988. Development of the Colle-Salvetti correlation-energy formula into a functional of the electron density. Phys. Rev. B. 37: 785. Ref.: shorturl.at/bsLQ7

DOI: https://doi.org/10.36811/jca.2020.110006 **JCA: August-2020: Page No: 10-21**

20. Keith TA, Bader RFW. 1993. Chem. Phys. Lett. 220: 223.
21. Keith TA, Bader RFW. 1992. Chem. Phys. Lett. 194: 1. Ref.: shorturl.at/eGHM5
22. Cheeseman JR, Frisch MJ, Trucks GW, et al. 1996. Chem. Phys. 104: 5497. Ref.: shorturl.at/aBX05